CANCER
COMMUNICATIONS Open Access

Inhibition of mTOR attenuates the initiation and progression of *BRCA1*-associated mammary tumors

Inherited mutation in breast cancer susceptibility gene 1 (*BRCA1*) is strongly associated with mammary tumors that exhibit triple-negative characteristics, are insensitive to endocrine-targeted therapies, and show basal-like properties, including aggressive phenotypes [1, 2]. It has been reported that the average cumulative risk of breast cancer for *BRCA1* mutation carriers by age 70 years is 57% (95% confidence interval [CI]: 47%-66%) [3]. Despite the high incidence and aggressive characteristics of *BRCA1*-associated breast cancer, few substantial improvements in preventing or treating this cancer have been made, largely due to the challenges of clinic-based cohort studies. During malignant transformation, cancer progression is facilitated by metabolic reprogramming–one of the hallmark characteristics of cancer. Previously, we found that inhibition of AKT is a potential strategy for the prevention and therapeutic management of *Brca1*-mutant mammary tumors. However, pharmacological inhibition proved less effective and less safe compared to genetic perturbation, limiting its potential for clinical application [4]. Meanwhile, mTOR, a key regulator of metabolism and a downstream target of the PI3K/AKT signaling pathway, has emerged as a promising therapeutic target for several diseases, including treatment of cancer [5].

In addition to identifying the contribution of mTOR signaling to BRCA1-deficient cells (Supplementary Figure S1), we provide genetic and pharmacological evidence using multi-orthogonal preclinical models [6–8] that mTOR is closely involved in the development and growth of *Brca1*-mutated mammary tumors (Figure 1A). To investigate the role of mTOR in the absence of BRCA1, we assessed the development of mammary glands in post-pubertal *Brca1/Mtor*-mutant mice by examining ductal and lobular development of the fourth mammary gland. Measurements of mammary gland density using the Branch software (ver. 1.1 [9]) showed that ductal length and branching were significantly diminished in the mammary glands of $Brca1^{co/co}Mtor^{co/co}MMTV$-*Cre* mice (Figure 1B,C, Supplementary Figure S2). To determine whether mTOR contributes to BRCA1-deficient mammary tumor formation, we examined tumor formation in cohorts of $Brca1^{co/co}$ ($n = 28$), $Brca1^{co/co}Mtor^{co/co}$ ($n = 30$), $Brca1^{co/co}MMTV$-*Cre* ($n = 24$), and $Brca1^{co/co}Mtor^{co/co}MMTV$-*Cre* ($n = 29$) mice (Top left of Figure 1A). $Brca1^{co/co}$ and $Brca1^{co/co}Mtor^{co/co}$ mice showed no signs of mammary abnormalities, including tumors, up to 24 months of age. In contrast, $Brca1^{co/co}MMTV$-*Cre* mutant mice developed breast cancer, reaching a high incidence (37.5%; 9/24) by 24 months of age. During the same period, $Brca1^{co/co}Mtor^{co/co}MMTV$-*Cre* mice exhibited a lower incidence of breast cancer (6.9%; 2/29) and significantly better tumor-free survival compared to $Brca1^{co/co}MMTV$-*Cre* mice ($P = 0.008$, log-rank test) (Figure 1D). Next, we examined whether mTOR inhibition using a clinically applicable pharmacological approach would produce similar effects as genetic ablation. To test pharmacological inhibition of mTOR, we administered everolimus (20 mg/kg, oral, 5 times/week) or vehicle to 4-month-old $Brca1^{co/co}MMTV$-*Cre* mice for 11 months (lower left of Figure 1A, Supplementary Figure S3). During this period, $Brca1^{co/co}MMTV$-*Cre* mice in both groups spontaneously developed palpable mammary tumors. At the end of the study period (15 months of age), vehicle-treated $Brca1^{co/co}MMTV$-*Cre* mice showed a high incidence of mammary tumors (93%; 13 of 14). During the same period, everolimus-treated $Brca1^{co/co}MMTV$-*Cre* mice exhibited a breast cancer incidence of 46% (5 of 11) and significantly longer tumor-free survival compared to their vehicle-treated counterparts ($P = 0.0117$, log-rank test) (Figure 1E). Moreover, while multiple tumors were found in 2 of 14 (14%) vehicle-treated mice, no cases of multiple tumors were detected in everolimus-treated mice (Figure 1F). In addition to tumor formation, whole-mount analysis of non-tumor–bearing mammary glands revealed

---

Hye Jung Baek, Geun Hee Han, and Eun Joo Cho contributed equally.

- -
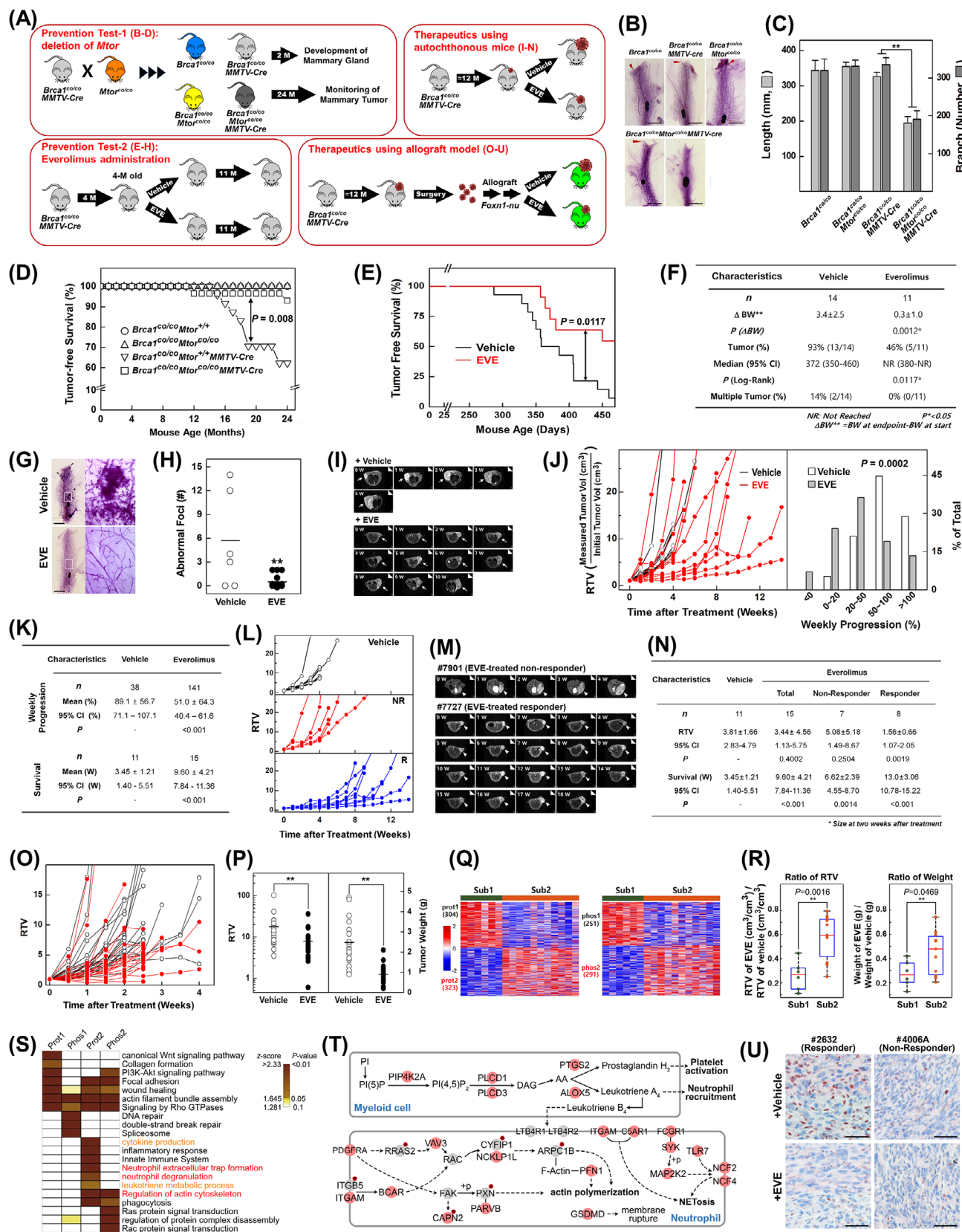
FIGURE 1 Contribution of mTOR in the initiation and progression of *BRCA1*-associated mammary tumors.

(A) Overview of the experimental designs to investigate the attenuation of tumor initiation and progression by mTOR inhibition in *Brca1*-mutant mice.

(B) Representative whole-mount staining of mammary glands from 2-month-old mice with the indicated genotypes. Arrows indicate the presence of sprouting ducts in the mammary glands. Scale bar, 5 mm.

that everolimus treatment reduced total ductal length and branch number by approximately 30% compared to vehicle treatment (Supplementary Figure S3). Notably, everolimus treatment significantly reduced the formation of abnormal hyperplastic foci (0.6 vs. 5.5 foci/mammary gland; $P < 0.01$) in non-tumor–bearing mammary glands of *Brca1*-mutant mice (Figure 1G,H). Taken together, these results suggest that genetic ablation and pharmacological inhibition of mTOR signaling prevents the proliferation of mammary epithelial cells and reduce tumor formation in *Brca1*-mutant mice.

To determine whether mTOR inhibition also suppresses the progression of *BRCA1*-associated breast cancer, we tested the efficacy of everolimus on spontaneously developed mammary tumors in *Brca1^{co/co}MMTV-Cre* mice through periodic observation and palpation. Tumor-bearing mice (size < 0.5 cm^3) were then randomized to receive either vehicle or everolimus via oral gavage (Top right of Figure 1A, Supplementary Figure S4). Tumor volumes at baseline and during progression were measured weekly using magnetic resonance imaging (MRI) until the tumors reached a volume of ∼3 cm^3 (Figure 1I).

(C) Total length (light gray) and branch numbers (dark gray) of ducts between the lymph node and the end tip in the 4th mammary glands of 2-month-old *Brca1^{co/co}* ($n = 9$), *Brca1^{co/co}Mtor^{co/co}* ($n = 16$), *Brca1^{co/co}MMTV-Cre* ($n = 18$), and *Brca1^{co/co}Mtor^{co/co}MMTV-Cre* ($n = 25$) mice, estimated using Branch software (***P < 0.01*, one-way ANOVA with Tukey's post hoc correction).

(D) Kaplan-Meier curves of tumor-free survival showing normal survival (100%) of *Brca1^{co/co}* ($n = 28$) and *Brca1^{co/co}Mtor^{co/co}* ($n = 30$) mice and significantly diminished tumor-free survival in *Brca1^{co/co}MMTV-Cre* mice ($n = 24$) compared with *Brca1^{co/co}Mtor^{co/co}MMTV-Cre* mice ($n = 29$) (**P = 0.008*, log-rank test).

(E-F) Kaplan-Meier curves (E) and Summary data (F) showing tumor-free survival of *Brca1^{co/co}MMTV-Cre* mice treated with vehicle ($n = 14$) or everolimus (EVE, $n = 11$, 20 mg/kg, oral, 5 times/week).

(G) Representative whole-mount staining of non-tumor-baring mammary glands from 15-month-old *Brca1^{co/co}MMTV-Cre* mice treated with vehicle or everolimus for 11 months. Small arrowheads indicate abnormal foci. The panels on the right are magnifications of the boxed areas in adjacent panels. Scale bar, 5 mm.

(H) Number of foci per mammary gland in vehicle- ($n = 6$) and everolimus-treated ($n = 11$) non-tumor-baring mammary glands (***P < 0.01*).

(I) Upon spontaneous tumor appearance, tumor-bearing mice were randomized into vehicle ($n = 11$) or everolimus ($n = 15$, 20 mg/kg, oral, 5 times/week) treatment. Tumor growth progression was monitored weekly by MRI. Representative MRI scans of tumor-bearing mice at baseline and following the indicated treatments.

(J) Graphs showing RTVs (left panel) between post-treatment and baseline (start of treatment) and analysis of weekly progression (right panel). Tumor growth was assessed by the RTV = tumor volume at a given time (cm^3)/tumor volume at the initiation of treatment (cm^3). Weekly progression in the everolimus-treated group was significantly lower than that in the vehicle-treated group ($P = 0.0002$, chi-square test).

(K) Summary data showing tumor progression and mouse survival following vehicle or everolimus treatment.

(L) Responsiveness of spontaneously developed mammary tumors from *Brca1^{co/co}MMTV-Cre* mice to everolimus, segregated based on mouse survival: non-responder (NR), survival ≤ 9 weeks; responder (R), survival > 9 weeks.

(M) Representative MRI scans of non-responder and responder tumor-bearing mice at baseline and the indicated times.

(N) Summary data showing everolimus-responsiveness of tumor progression (RTV) and mouse survival.

(O) Graph showing calculated RTVs for engrafted tumors treated with vehicle (black lines) or everolimus (red lines). Spontaneously developed mammary tumors ($n = 22$) were collected from *Brca1^{co/co}MMTV-Cre* mice and transplanted into nude mice. Growth of the corresponding tumors in sham-treated mice versus mice treated with everolimus (5 mg/kg, oral, 5 times/week) was tested. All mice were sacrificed when any tumors from a shared origin reached ∼3 cm^3.

(P) Comparison of RTVs and tumor weights at the end of the study between vehicle-treated ($n = 22$) and everolimus-treated ($n = 22$) mice.

(Q) Heat maps showing protein (prot1 and prot2) and phosphopeptide (phos1 and phos2) signatures (rows) defining Sub1 and Sub2. The numbers of proteins and phosphopeptides are indicated in parentheses.

(R) Box plots showing ratios of RTVs (left panel) and tumor weights (right panel) at endpoints in everolimus-treated samples compared with their paired vehicle-treated samples in Sub1 and Sub2. **, $P < 0.01$; *, $P < 0.05$ from two-sample t-test.

(S) Cellular pathways significantly enriched by proteins (prot1 and 2) and phosphoproteins of selected phosphopeptides (phos1 and phos2) defining Sub1 and Sub2. The heat map shows pathway enrichment significance, represented as z-scores computed as $-N^{-1}(P\text{-value})$, where P-value is the enrichment P-value from DAVID or ConsensusPathDB, and $N^{-1}(P\text{-value})$ is the inverse normal distribution.

(T) Network model showing interactions between proteins and phosphorylated proteins involved in leukotriene metabolic process (top), actin cytoskeleton regulation (bottom left), and neutrophil extracellular trap formation (NETosis, bottom right). Pink nodes indicate proteins (prot2) defining Sub2, while circled P on a node indicates phosphoproteins containing the phosphopeptides (phos2) defining Sub2. Solid arrows indicate direct activation; dotted arrows indicate indirect activation; arrows with "+p" denote phosphorylation.

(U) Representative immunohistochemistry images of ALOX5 for the indicated responder and non-responder. Scale bar, 50 μm.

Abbreviations: AA, arachidonic acid; DAG, diacylglycerol; PI, phosphatidylinositol.

Tumors in vehicle-treated mice grew more rapidly than those in everolimus-treated mice (Figure 1J, left panel). An analysis of weekly progression showed that 73% (28 of 38) of tumors in vehicle-treated mice exhibited greater than 50% progression, compared to only 33% (46 of 141) in everolimus-treated mice (Figure 1J, right panel; $P = 0.0002$, chi-square test). Additionally, the weekly increase in tumor volume in the everolimus-treated group (51.0%, 95% CI: 40.3%-61.8%) was significantly lower ($P < 0.001$) than that in the vehicle-treated group (89.1%, 95% CI: 70.4%-107.7%). Moreover, everolimus-treated mice showed significantly longer survival (2.8-fold on average) compared to vehicle-treated mice (Figure 1K; $P < 0.001$). Importantly, while everolimus treatment significantly improved therapeutic outcomes in *Brca1*-mutant tumors, responses to everolimus showed heterogeneity among individual mice. Specifically, 8 of the 15 mice, designated as responder mice, exhibited a significant reduction in the ratio of tumor volume (RTV) in response to everolimus. In contrast, the remaining 7 mice, designated as non-responders, displayed a higher RTV than responders and vehicle-treated mice (Figure 1L,M). Additionally, the survival of responders (13.0 weeks) was nearly double that of non-responders (6.6 weeks) (Figure 1N). To further examine the therapeutic efficacy of everolimus, we employed an engraft model for preclinical evaluation. Tumor tissues were collected from 22 individual spontaneously developed mammary tumors in *Brca1^{co/co}MMTV-Cre* mice, orthotopically transplanted into nude female mice, amplified, re-transplanted, and subsequently treated with either vehicle or everolimus. Tumor progression was monitored (bottom right of Figure 1A, Supplementary Figure S5), and all mice were sacrificed when any tumors in either vehicle- or everolimus-treated group reached ~3 cm^3 (Figure 1O, Supplementary Figure S6). Tumors from everolimus-treated mice showed significant reductions in RTV (43%) and weight (38%) compared to tumors from vehicle-treated mice (Figure 1P, Supplementary Figure S5). These findings suggest effective management of *BRCA1*-associated breast cancer by pharmacological mTOR inhibition.

To explore this heterogeneity, we conducted global proteome and phosphoproteome profiling of vehicle- and everolimus-treated allograft tumors (Supplementary Figure S7A). Two distinct sample clusters (Sub1 and Sub2) were identified using both protein and phosphopeptide data (Supplementary Figure S7B,C). We identified 304 and 323 proteins that were upregulated, and 251 and 291 phosphopeptides that were upregulated, in Sub1 and Sub2, respectively (Figure 1Q). Sub2, characterized by higher RTVs and weights, represented the non-responders, whereas Sub1 corresponded to the responders (Figure 1R). The upregulated proteins and phosphopro-teins in Sub2 were associated with neutrophil extracellular trap formation (NETosis) and leukotriene metabolism (Figure 1S). Enzymes involved in phosphatidylinositol and arachidonic acid formation/metabolism were upregulated in non-responders, leading to the release of leukotrienes (Figure 1T). Upon leukotriene binding, (1) proteins and phosphorylations mediating actin polymerization required for neutrophil migration, and (2) proteins involved in NETosis, were upregulated in non-responders (Figure 1T). Western blotting and immunohistochemistry confirmed the upregulation of representative markers of the leukotriene and NETosis pathways (Figure 1U, Supplementary Figure S7D,E).

Therefore, our findings provide preclinical evidence that targeting mTOR inhibition is a potential strategy for the prevention and therapeutic management of *BRCA1*-associated breast cancer. Additionally, activation of the leukotriene-neutrophil activation axis can serve as a predictive marker of resistance to targeted mTOR inhibition. We further discussed the leukotriene signaling as a predictive biomarker and potential clinical translational value of this study in supplementary information.

AUTHOR CONTRIBUTIONS

Chang-il Hwang, Daehee Hwang, and Sang Soo Kim conceived the study, designed, and supervised the experiments. Tae Hyun Kim, Chu-Xia Deng, Sung Chul Lim, Chang-il Hwang, Daehee Hwang, and Sang Soo Kim wrote and revised the manuscript. Eun Jung Park, Tae Hyun Kim, Dong Hoon Shin, Heesun Cheong, Chu-Xia Deng, Sung Chul Lim, Chang-il Hwang, Daehee Hwang, and Sang Soo Kim contributed to the data analysis and interpretation. Hye Jung Baek, Jihao Xu, and Heesun Cheong contributed to the in vitro experiments. Eun Joo Cho, Min Kyung Ki, and Dong Hoon Shin conducted the in vivo animal experiments. Geun Hee Han performed bioinformatical analysis. Tae Hyun Kim executed the statiscal analysis. Sung Chul Lim performed the pathological analysis. Eun Jung Park performed immunological analysis. All authors read and approved the final manuscript.

ACKNOWLEDGEMENTS

CONFLICT OF INTEREST STATEMENT

The authors declare no conflict of interest.

FUNDING INFORMATION

DATA AVAILABILITY STATEMENT

All generated global and phosphoproteomic data have been deposited in the ProteomeXchange Consortium (http://proteomecentral.proteomexchange.org) via the PRIDE partner repository, with PXD054301 as the identifier [10].

ETHICS APPROVAL AND CONSENT TO PARTICIPATE

All procedures involving animals and their care were approved by the Institutional Animal Care and Use Committee of the National Cancer Center of Korea (NCC-15-295).

Hye Jung Baek[1]
Geun Hee Han[2]
Eun Joo Cho[1]
Jihao Xu[3]
Min Kyung Ki[1]
Eun Jung Park[1]
Tae Hyun Kim[1]
Dong Hoon Shin[1]
Heesun Cheong[1]
Chu-Xia Deng[4]
Sung Chul Lim[5]
Chang-il Hwang[3]
Daehee Hwang[2,6]
Sang Soo Kim[1]

[1]Research Institute, National Cancer Center, Goyang, South Korea
[2]School of Biological Sciences, Seoul National University, Seoul, South Korea
[3]Department of Microbiology and Molecular Genetics, College of Biological Sciences, University of California, Davis, USA
[4]Cancer Centre, Faculty of Health Sciences, University of Macau, Macau, P. R. China
[5]Department of Pathology, College of Medicine, Chosun University, Gwangju, South Korea
[6]SNU Bioinformatics Institute, Seoul National University, Seoul, South Korea

Correspondence

Sang Soo Kim, Research Institute, National Cancer Center, Goyang 10408, Republic of Korea.
Email: sangsookim@ncc.re.kr

Daehee Hwang, School of Biological Sciences, Seoul National University, Seoul 08826, Republic of Korea.
Email: daehee@snu.ac.kr

Chang-il Hwang, Department of Microbiology and Molecular Genetics, College of Biological Sciences, University of California, Davis, CA 95616, USA.
Email: cihwang@ucdavis.edu

ORCID

Chu-Xia Deng https://orcid.org/0000-0001-8033-3902
Sang Soo Kim https://orcid.org/0000-0002-4079-2503

REFERENCES

1. Venkitaraman R. Triple-negative/basal-like breast cancer: clinical, pathologic and molecular features. Expert Rev Anticancer Ther. 2010;10(2):199–207.
2. Nanda R. "Targeting" triple-negative breast cancer: the lessons learned from BRCA1-associated breast cancers. Semin Oncol. 2011;38(2):254–262.
3. Chen S, Parmigiani G. Meta-analysis of BRCA1 and BRCA2 penetrance. J Clin Oncol. 2007;25(11):1329–1333.
4. Baek HJ, Kim SE, Kim JK, Shin DH, Kim TH, Kim KG, et al. Inhibition of AKT suppresses the initiation and progression of BRCA1-associated mammary tumors. Int J Biol Sci. 2018;14(13):1769–1781.
5. Zou Z, Tao T, Li H, Zhu X. mTOR signaling pathway and mTOR inhibitors in cancer: progress and challenges. Cell Biosci. 2020;10:31.
6. Xu X, Wagner KU, Larson D, Weaver Z, Li C, Ried T, et al. Conditional mutation of Brca1 in mammary epithelial cells results in blunted ductal morphogenesis and tumour formation. Nat Genet. 1999;22(1):37–43.
7. Wagner KU, Wall RJ, St-Onge L, Gruss P, Wynshaw-Boris A, Garrett L, et al. Cre-mediated gene deletion in the mammary gland. Nucleic Acids Res. 1997;25(21):4323–4330.
8. Risson V, Mazelin L, Roceri M, Sanchez H, Moncollin V, Corneloup C, et al. Muscle inactivation of mTOR causes metabolic and dystrophin defects leading to severe myopathy. J Cell Biol. 2009;187(6):859–874.
9. Baek HJ, Kim SE, Choi EK, Kim JK, Shin DH, Park EJ, et al. Inhibition of Estrogen Signaling Reduces the Incidence of BRCA1-associated Mammary Tumor Formation. Int J Biol Sci. 2018;14(12):1755–1768.
10. Vizcaíno JA, Deutsch EW, Wang R, Csordas A, Reisinger F, Ríos D, et al. ProteomeXchange provides globally coordinated proteomics data submission and dissemination. Nat Biotechnol. 2014;32(3):223–226.

SUPPORTING INFORMATION

Additional supporting information can be found online in the Supporting Information section at the end of this article.